

Study of scattering material with RadioAstron-VLBI observations

T.V. Smirnova, V.I. Shishov, M.V. Popov, C. Gwinn, J. Anderson, A.S. Andrianov, N. Bartel, A. Deller, M. Johnson, B.C. Joshi, N.S. Kardashev, R. Karuppusamy, M. Kramer, A. Rudnitsky, Y. Safutdinov, V.I. Soglasnov

The RadioAstron spacecraft presents a unique opportunity to measure properties of interstellar scattering. The fluctuations responsible for scattering radio waves from astronomical sources are small-scale (~ 0.1 AU) fluctuations in the electron offer a variety of observables for interstellar scattering. Observations of density of the interstellar medium. Pulsars scattering of nearby pulsars and intra-day variable quasars point to the existence of a component of the interstellar medium (ISM) which has properties quite different from the more distant, diffuse ISM. We observed several nearby pulsars as part of RadioAstron's Early Science Program (ESP). These included pulsars B0950+08 and B1919+21. We present here results concerning the distribution and properties of scattering material in the direction to these pulsars obtained with cosmic interferometer.

Introduction

The RadioAstron spacecraft presents an unique opportunity to measure properties of interstellar scattering. The fluctuations responsible for scattering radio waves from astronomical sources are small-scale (~ 0.1 AU) fluctuations in the electron density of the interstellar medium. Pulsars offer a variety of observables for interstellar scattering. The time series of electric field emitted by the pulsar is convolved with an impulse-response function due to scattering, when sampled at the observer plane. This impulse-response function reflects the reinforcement or cancellation of radiation that has traveled along different lines of sight, as deflected by the propagation medium. The impulse-response function has a typical timescale t_{diff} , reflecting the range of travel times from source to observer. The bandwidth of scintillations $\Delta\nu_s = 1/2\pi t_{diff}$ is the range of frequencies for which the cancellation or reinforcement persists. The impulse-response function has a characteristic scale in the observer plane S_{ISS} that reflects the relative variations in the path lengths as the position of the observer changes. The angular scale of the scattering disk - the region on the sky from which the observer receives radiation - is $\theta_{scat} = \lambda/S_{ISS}$, where λ is the observing wavelength. For transverse velocity of the pattern V , the timescale of scintillation is $t_s = S_{ISS}/V$. Our first scientific results obtained with Cosmic-Earth interferometer were published in ApJ [1]. We studied there the distribution of scattering material in the line of sight to PSR B0950+08.

Main relations

Scattering convolves the electric field of the source with an impulse-response function $g(t)$: $E_{obs}(t) = g(t) \otimes E_{source}(t)$. The impulse-response function $g(t)$ varies over a lateral scale $S_{ISS} \sim$ few radius of the Earth, R_E . $g(t)$ changes as the Earth moves across the observer plane. The cross-power spectrum is the product of Fourier transforms of the impulse-response functions getting from two telescopes A and B: $V_{AB}(\omega) = g_A(\omega) g_B^*(\omega)$. If the baseline is much shorter than S_{ISS} , $g(\omega)$ is the same at both antennas, and V_{AB} is real and positive. If the baseline is much longer than S_{ISS} , impulse-response functions are completely different at the two antennas and phase of V_{AB} varies randomly between π and $-\pi$. Amplitude of V_{AB} is a dynamic spectrum of pulsar: intensity of signal as a function of frequency and time. In Fig. 1 we present the dynamic spectra of PSR B1919+21 obtained from our observation for Green Bank-Westerbork baseline. Spatial spectra of plasma inhomogeneities is defined by: $\Phi_g(\mathbf{q}) \propto |\mathbf{q}|^{-\alpha+2}$, $\mathbf{q} = 2\pi/\lambda$ is a spatial frequency. Structure function (SF) of phase fluctuations is: $D_{\phi}(\Delta\mathbf{p}) = \langle (\psi(\mathbf{p}) - \psi(\mathbf{p} + \Delta\mathbf{p}))^2 \rangle$, where \mathbf{p} is a spatial coordinate in the observer plane and $\Delta\mathbf{p}$ is a baseline of interferometer. As it was shown in [1] for weak scintillation we have, $SF = [D(\mathbf{p} + \mathbf{p}_1 + \mathbf{p}_2) + D(\mathbf{p} - \mathbf{p}_1 - \mathbf{p}_2) + 2D(\mathbf{p}_1 + \mathbf{p}_2) - 4D(\mathbf{p})]$. If we have two phase changing screens located at distances z_1 and z_2 then $D_{\phi}(\mathbf{p}) = k(\theta_{scat}, |\mathbf{p}|)^\alpha$, $\alpha = (1, 2)$. In presence of cosmic prism in the line of sight we will have deflection radiation from the pulsar at a frequency-dependent refractive angle, θ_{ref} . If refractive angle is significantly greater than the scattering angle at either screen: $|\theta_{ref}| \gg \theta_{scat}$, then displacement of the source will be: $\theta_s = 2(\Delta f/f_0)\theta_{ref}$ and displacement of the scintillation pattern for two layers for case $z_1 \ll z_2$ will be: $\rho_{1,1} = z_1\theta_s$, $\rho_{1,2} = V_{obs}^* \Delta t$, $\rho_{2,2} = z_2/z_1(z_2 - z_1)\theta_s$, $\rho_{2,1} = V_2^* \Delta t$, V_2 is a combination of observer, pulsar and screen velocities: V_{obs} , V_{psr} , V_{scr} . Structure function of intensity variations is: $D_{\Delta I}(\Delta\mathbf{p}, f, t) = \langle (\Delta I(\mathbf{p} + \Delta\mathbf{p}, f, t) - \Delta I(\mathbf{p}, f, t))^2 \rangle$.

Observations and data reduction, analysis of data

Frequency 316 MHz, Bandwidth 16 MHz, total duration time is about 1h. Data were correlated with the ASC correlator, gating and dedispersion. We used telescopes: RadioAstron (RA), Arecibo (AR), Westerbork (WB) for B0950+08 and RA, WB and GB (Green Bank) for PSR B1919+21. Data were recorded in 560 s scans with 30 s gaps between scans. On-pulse window includes intensities inside of mean profile on its 0.3 amplitude level. The off-pulse window was offset from the pulse by half of period.

PSR B0950+08: 25.01.2012, Projection of base is 220000 km, observing time 1 h
DM = 2.97, Z = 262 pc, $P_1 = 0.253$ s, time resolution was $\Delta t = 1$ s ($4P_1$ averaging) and $\Delta f = 125$ kHz (128 channels).

PSR B 1919+21: 04.07.2012, Projection of base is 60000 km, observing time 69.5 min
DM = 12.43, Z = 1.1 kpc, $P_1 = 1.337$ s, time resolution, $\Delta t = 5.35$ s ($4P_1$ averaging) and $\Delta f = 31.25$ kHz (512 channels).

To analyze diffraction pattern in on-pulse radio spectra we averaged cross-spectra over $4P_1$, and then applied corrections for receiver bandpass using off-pulse spectra. We also normalized cross-spectra by mean intensities over spectra to decrease influence of strong pulse-to-pulse intensity fluctuations. Analysis of dynamic spectra gave us scintillation time, t_s and decorrelation bandwidth, f_d . The visibility functions were computed as the inverse Fourier transform of the complex cross-spectra. Module of cross-spectra averaged over time give us interferometric visibility or coherence function. A mean structure function (SF) is defined using intensities in square to decrease influence of noise: $SF(\Delta f, \Delta t) = \langle |I^2(f, t) - I^2(f + \Delta f, t + \Delta t)|^2 \rangle_{t, t'}$. SF for the squared modulus of the visibility is proportional to the structure function for the modulus of visibility. Mean structure functions for different time lags Δt on the AR-WB baseline (left) and RA-AR baseline (right) are shown in Fig. 2 and Fig.3 for PSR 0950+08 and B1919+21 correspondently. The numbers in figures correspond to the time shift Δt in s. SF's shown in Fig.2 and Fig.3 for both pulsars have qualitatively different forms. We see that for both pulsars structure functions have two scales. Short baseline comprises a narrow-bandwidth component and a broader-bandwidth component. For the long RadioAstron-Arecibo or GB space baseline, the narrow-bandwidth component is absent, we see only the broad-bandwidth structure for PSR B0950+08. The long baseline suppresses most of the narrowband structure and some of the wideband structure for PSR B1919+21. Shows that for this pulsar cosmic interferometer resolves the small-scale structure.

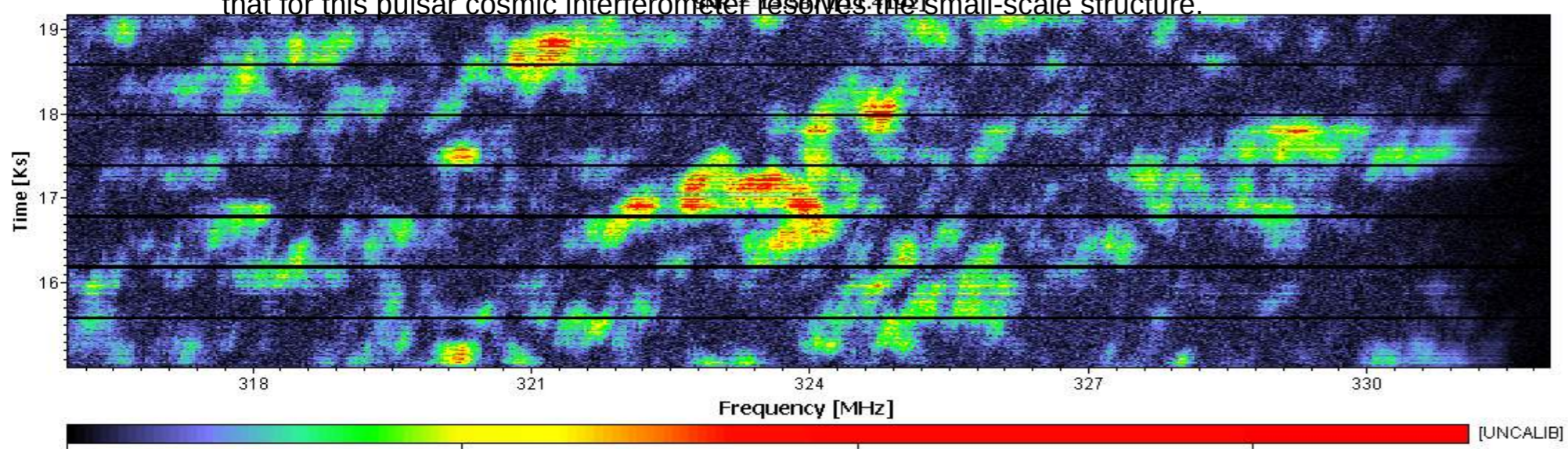


Fig.1. Dynamic spectra of PSR B1919+21 on the GB-WB baseline

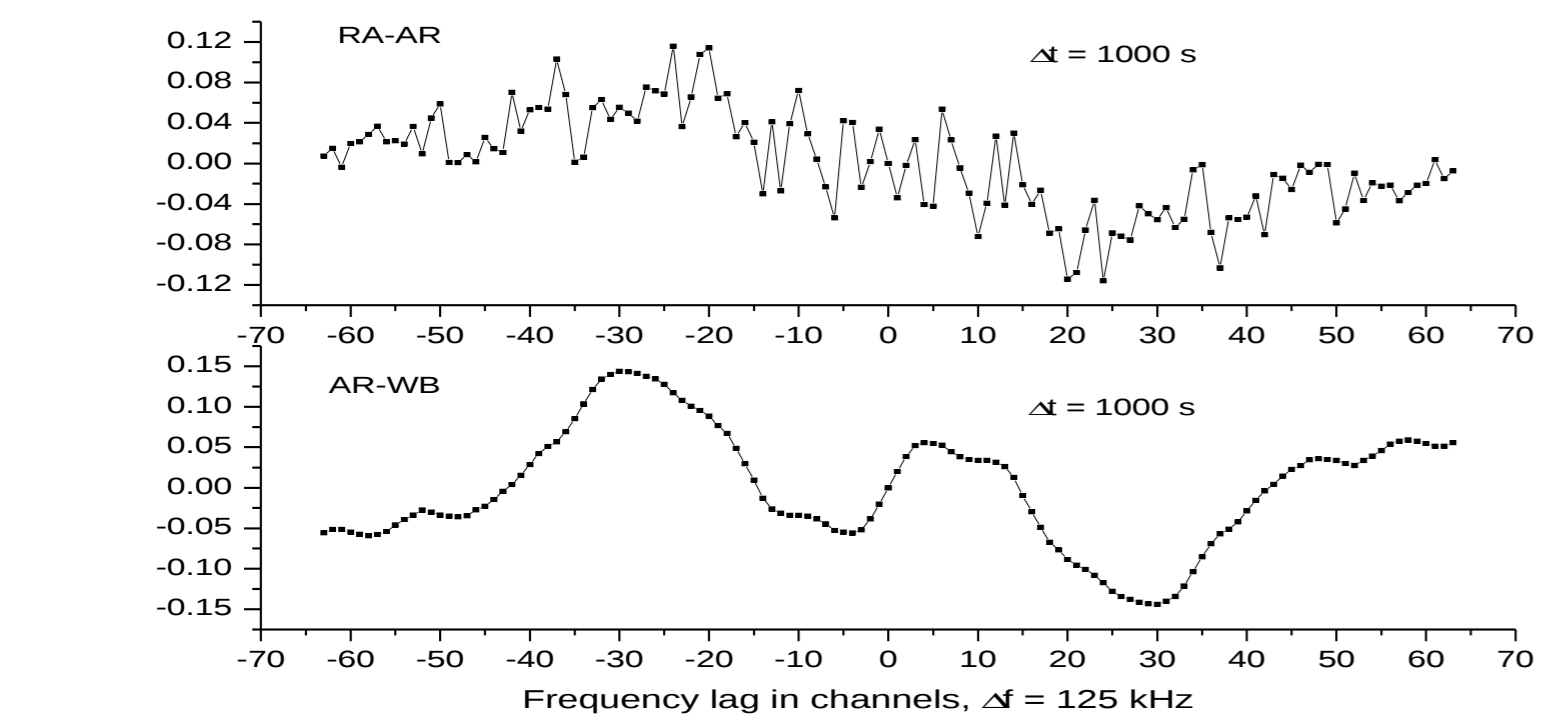


Fig.4. Structure functions difference for positive and negative frequency lags for B0950+08

The narrower component also appears only at small time lags: less than 1000s for PSR B0950+08 and about 250 s for PSR B1919+21, whereas the broader component appears at both large and small time lags. The two frequency scales (3.1 MHz and more or about 8 MHz for B0950+08; 0.3 MHz and 2 MHz for PSR B1919+21) correspond to two effective layers of turbulent plasma, separated in space, where scattering of pulsar emission take place. For PSR B0950+08 we have a weak scintillation regime - modulation index is about 0.4. For this case we can use a simple model for the shorter baseline structure function as a sum of SF's corresponded to the two screens. We defined modulation indices for two screens as $0.32 < m_1 < 0.43$ and $m_2 = 0.15$ for the nearby and the distant layers correspondently. The range of limits for m_1 is defined by uncertainty of the Fresnel frequency scale: $f_{Fr,1} = 8 - 16$ MHz.

We can use the behavior of the structure function with time, as well as frequency, to estimate the Fresnel scales and distances of the scattering screens. The amplitude of the narrower component of the structure function decreases with increasing time shift, and falls to zero at time lag $\Delta t = 1000$ s. We evaluated Fresnel scales and distances to both screens as: $\rho_{Fr,1} = (1.4 \text{ to } 2.7) \times 10^5$ km, $z_1 = k(\rho_{Fr,1})^2 = (4.4-16.4)$ pc; $\rho_{Fr,2} = (3.5 \text{ to } 15) \times 10^5$ km, $z_2 = (26-170)$ pc. We can evaluate the refractive angle as: $\theta_0 = \rho_{Fr,1} v_0 / (2z_1 f_{Fr,1}) = (1.1-4.4)$ mas.

The cosmic prism disperses the scintillation pattern across the observer plane, so that particular intensity maxima and minima appear at different positions at different frequencies. The shift in frequency of the scintillation pattern with a time or position leads to an asymmetry in frequency Δf of the structure function: $SF(\Delta f, \Delta t, \Delta p)$, for nonzero time lag (Δt) or finite baseline length, Δp . Asymmetry function we calculated as: $SF(\Delta f, \Delta t) - SF(-\Delta f, \Delta t)$. In Fig. 4 and Fig.5 we show these asymmetry functions for PSR B0950+08 and B1919+21. We can estimate directions of refractive dispersion and screen velocity from the measured asymmetry of the structure function. For our observations on the short Arecibo-Westerbork baseline, the weak asymmetry of the structure function, along with a relatively rapid decorrelation of the narrow component at $\Delta t = 1000$ s as seen in Figure 2 (left), suggests that the angle between the vectors θ_0 and observer velocity, V_{obs} is close to $\pi/2$. We obtained the power index of the power spectra of plasma density inhomogeneities for PSR B0950+08 using the mean coherence function (see Fig. 6). This index differs strongly from Kolmogorov value of $\gamma = 11/3$.

Interstellar scintillation of PSR B1919+21 is defined by two components: one causes diffractive scintillation with the frequency scale of $\Delta f_1 = 0.3$ MHz and the time scale of $t_{diff} = 250$ s. It is located at distance z_1 . An other one is located at distance z_2 near to observer and causes a weak scintillation of pulsar emission with the frequency scale of $\Delta f_2 = 2$ MHz (Fig.3). We evaluated the mean amplitude of visibility function in square as $|V(\mathbf{p})|^2 = 0.05$. In the regime of strong scintillation and power spectra of inhomogeneities we have a relation: $|V(\mathbf{p})|^2 = \exp[-(p/r_{diff})^\alpha]$. We got $\alpha = 1$ from the shape of structure function, so $r_{diff} = 1/3p = 2 \times 10^9$ cm. Scattering angle is $\theta_{diff} \approx 1.5$ mas and it is resolved by cosmic interferometer. The pulsar velocity, V_{psr} , is 200 km/s. In the plane of observer we have $r_{diff} / V_{psr} t_{diff} = 2/5$, $z_1 = (2/7)z = 0.3$ kpc from observer. From the shape of asymmetry function we can conclude that the base of cosmic interferometer is about the scale of the second component: $r_{weak} = (z_2/k)^{1/2} \approx \rho = 6 \times 10^9$ cm. So we have $z_2 = k\rho^2 = (2/3)$ pc.

The frequency scale of refractive scintillation is defined by: $\theta_{ref} = \theta_{diff} [2(\Delta f_1/f)] \approx 75\theta_{diff} \approx 100$ mas. The frequency scale of diffractive scintillation is defined by: $2(\Delta f_1/f)_{pr} \theta_{ref} = r_{diff}$, where r_{diff} is the distance of prism from the observer. Using this relation we get: $z_2 \approx (5/3)$ pc.

PSR B0950+08: We detected the presence of two scattering plasma layers along the line of sight to the pulsar. Modulation index is mainly defined by nearby layer. From analysis of the time and frequency parameters of scintillation, we found that screens are located at distances of 4.4-16.4 pc, and of 26-170 pc, respectively. The nearby layer dominates the temporal structure of the scintillation, while both the nearby and far layers influence the frequency structure of the scintillation. Its scattering shows similarities to that of intra-day variable extragalactic sources. We observe evidence for refraction by an interstellar plasma wedge, or "cosmic prism." For PSR B0950+08, we evaluated the angle of refraction as $\theta_0 = (1.1-4.4)$ mas. The spectra of density fluctuations for the two layers were found to follow power laws, with indices $\gamma_1 = \gamma_2 = 3.00 \pm 0.08$. These indices differ from the Kolmogorov value of $\gamma = 11/3$.

PSR B1919+21: Interstellar scintillation of PSR B1919+21 is defined by two screens of plasma inhomogeneities. Frequency structure of scintillation is defined by angular refraction of the cosmic prism located on the distance of 1.7 pc. We defined refractive angle as 100 mas. Cosmic interferometer resolves the scattering disk, the size of it: $\theta_{diff} \approx 1.5$ mas. We detected the locations of two screens which are 0.7 pc and 300 pc.

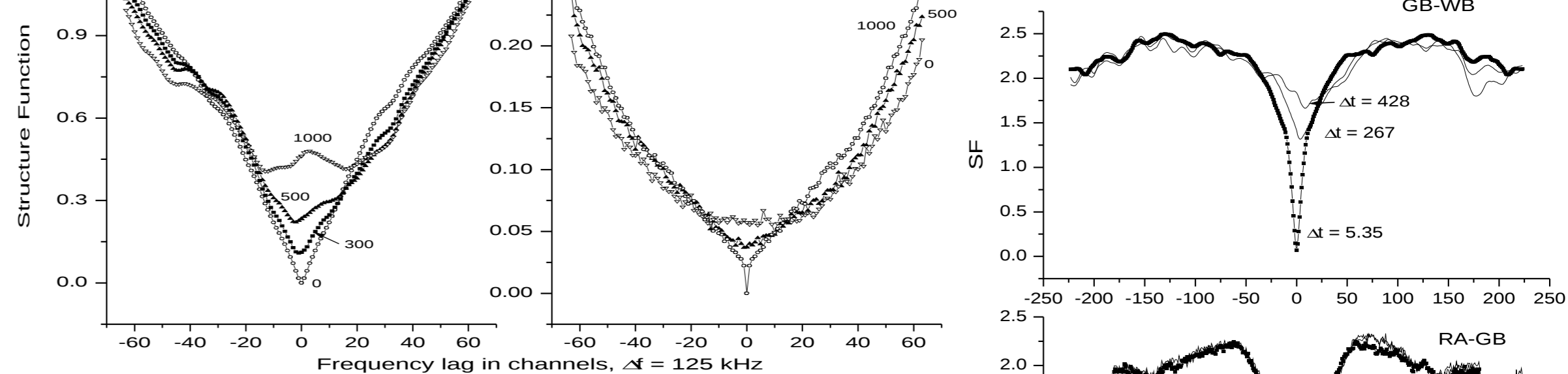


Fig. 2 and Fig.3: Structure functions for two baselines. The numbers show the time shift in s

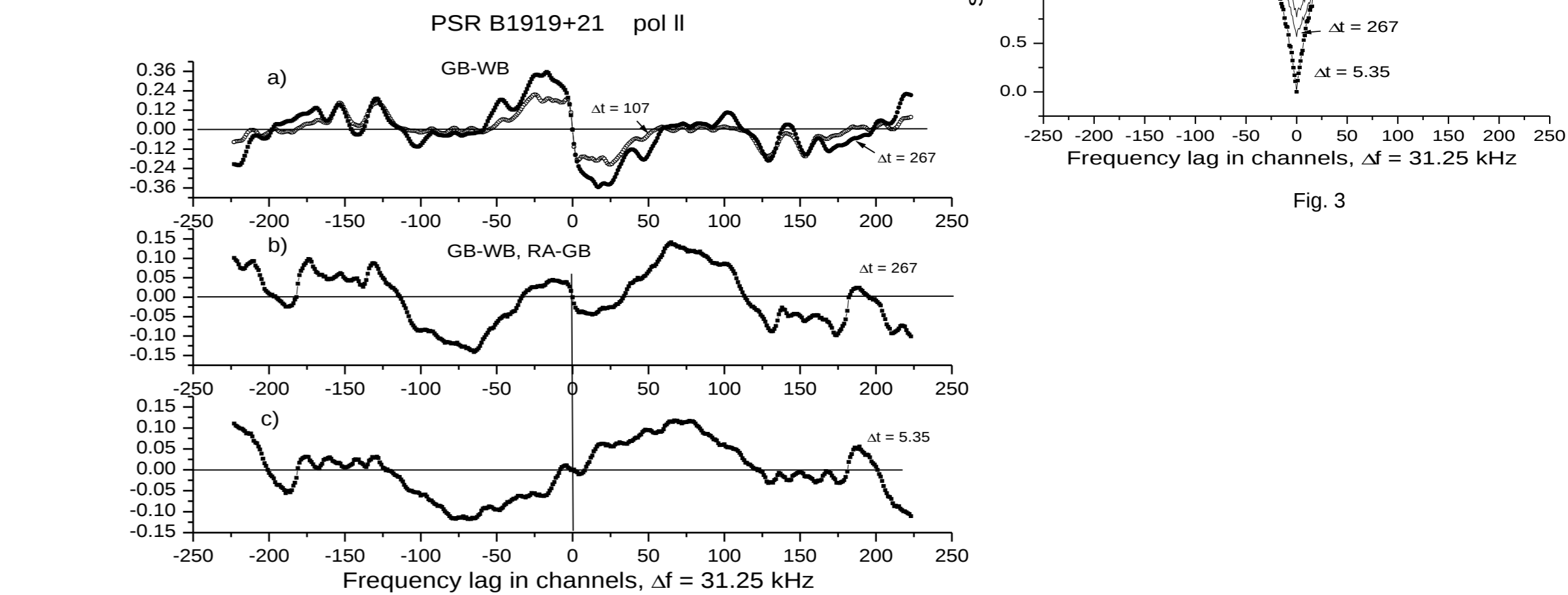


Fig. 5. Asymmetry functions for: a) Green Bank - Westerbork (GB-WB) baseline; b) and c) between cosmic (RA-GB) and Green Bank - Westerbork baselines. The numbers show the time shift in s.

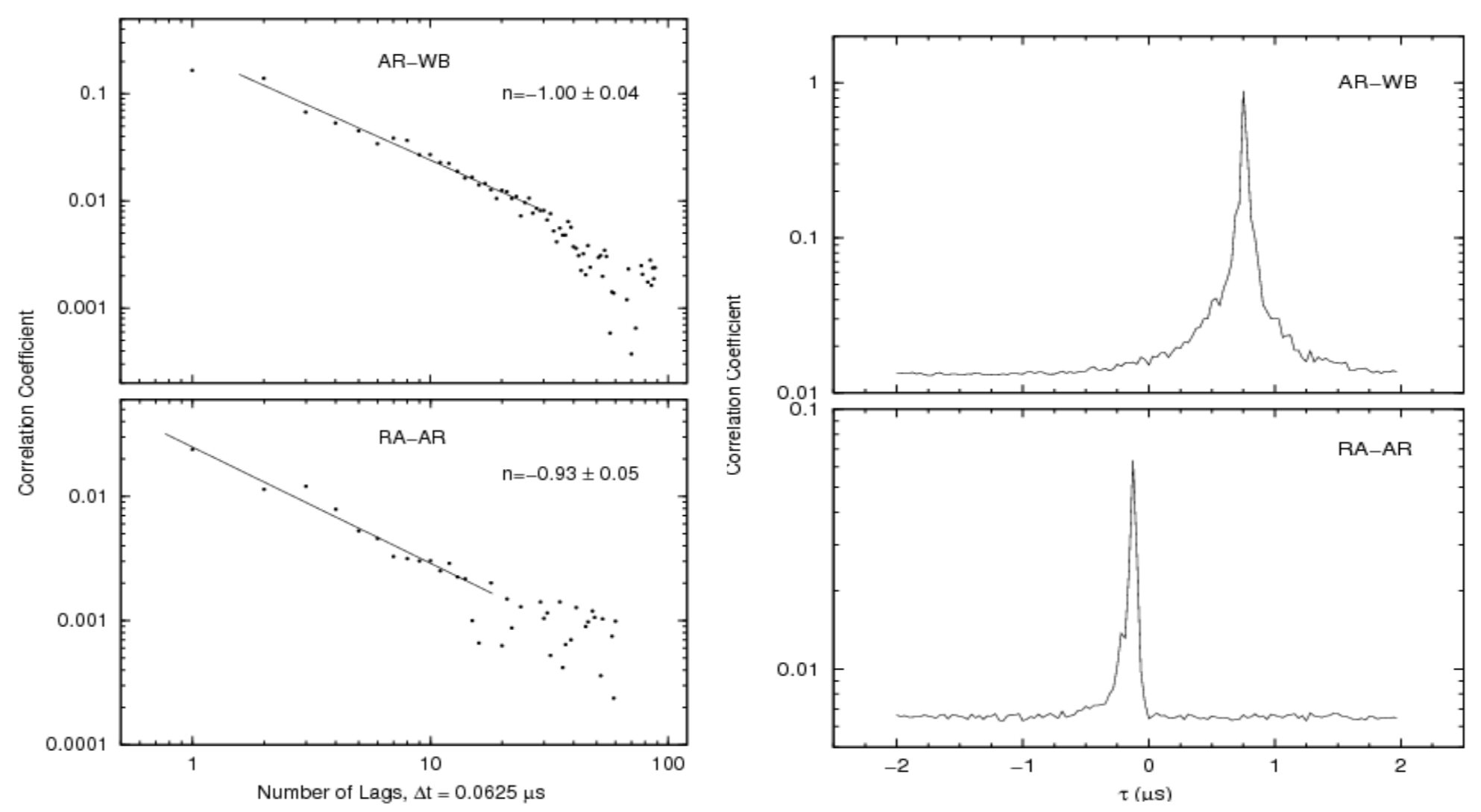


Fig. 6. Mean coherence function for PSR B0950+08 (right side): for the Arecibo-Westerbork (top), and RadioAstron-Arecibo baselines (bottom). The y-axis is amplitude plotted on a log scale. Left side: Leading part of the coherence function shown on a log-log scale. The noise level has been subtracted. Straight lines correspond to a power-law fit using points not contaminated by noise. The slope $n = -1$ corresponds to an index of $\gamma_1 = \gamma_2 = 3.00$ for spectra of density fluctuations.